

# Accurate Gas-Phase Experimental Structures of Octasilsesquioxanes (Si<sub>8</sub>O<sub>12</sub>X<sub>8</sub>; X = H, Me)

Derek A. Wann,<sup>†</sup> Robert J. Less,<sup>‡</sup> Franck Rataboul,<sup>‡</sup> Philip D. McCaffrey,<sup>†</sup> Anthony M. Reilly,<sup>†</sup> Heather E. Robertson,<sup>†</sup> Paul D. Lickiss,<sup>‡</sup> and David W. H. Rankin<sup>\*†</sup>

School of Chemistry, University of Edinburgh, West Mains Road, Edinburgh, U.K. EH9 3JJ, and Department of Chemistry, Imperial College London, South Kensington, London, U.K. SW7 2AZ

Received April 21, 2008

The accurate structures of silsesquioxanes Si<sub>8</sub>O<sub>12</sub>H<sub>8</sub> and Si<sub>8</sub>O<sub>12</sub>Me<sub>8</sub> have been determined by gas-phase electron diffraction methods in order to obtain experimental data on single molecules unconstrained by a crystal lattice for comparison with data obtained by theoretical methods. For Si<sub>8</sub>O<sub>12</sub>H<sub>8</sub> the experimentally determined structure shows ideal *O<sub>h</sub>* symmetry with Si–O distances and Si–O–Si angles of 161.41(3) pm and 147.9(2)° [*r<sub>e</sub>*, uncertainties (*σ*) in parentheses] compared with 162.9 pm and 147.8° for theoretical results from MP2/6-311++G(3df,3pd) calculations. In Si<sub>8</sub>O<sub>12</sub>Me<sub>8</sub> a similar *O<sub>h</sub>* symmetry model gave experimental values of 161.74(5) pm and 148.9(2)° for the Si–O distances and Si–O–Si angles compared with calculated values of 163.2 pm and 148.6°, respectively.

## Introduction

Octahydridosilsesquioxane (Si<sub>8</sub>O<sub>12</sub>H<sub>8</sub>) and its octamethylated analogue octamethylsilsesquioxane (Si<sub>8</sub>O<sub>12</sub>Me<sub>8</sub>) are part of a wider class of molecules known as polyhedral oligomeric silsesquioxanes (POSS). These are nanometer-sized, multifunctional molecules with a general chemical composition (XSiO<sub>1.5</sub>)<sub>*n*</sub>, where *n* can take values 4, 6, 8, 10, etc., and X can vary widely. POSS systems have a range of potential and actual applications including as additives to alter the physical and chemical properties of many everyday materials such as paints, coatings, packaging materials, resins, elastomers, and advanced plastics.<sup>1–3</sup> They are also suitable for modifying interfacial properties<sup>4</sup> and have been shown to be useful for modeling catalysts<sup>5</sup> and when included in metal complexes, as actual olefin polymerization catalysts.<sup>6</sup> Their use as nanoscale building blocks<sup>7,8</sup> has been demonstrated, as has their ability to produce water-soluble micelles,<sup>9,10</sup> nanocomposite foams,<sup>11,12</sup> liquid crystals,<sup>13–15</sup> and

CVD coatings.<sup>16</sup> They have also provided a route to synthesizing hyperbranched or cross-linked polymers.<sup>3,17–21</sup> In addition, the cubic Si<sub>8</sub>O<sub>12</sub> fragment is well known as the double 4-ring unit in inorganic framework materials such as zeolites.<sup>22</sup>

This remarkable array of applications stems from the rich chemistry that arises due to the wide range of substituents that can be accommodated at the Si vertices of the POSS and the ease with which they can be modified and elaborated. The POSS cores are also relatively chemically and thermally stable, allowing robust materials to be made. The chemistry of a wide range of POSS derivatives has been reviewed.<sup>20h,23</sup>

Structurally, the most widely investigated POSS is octahydridosilsesquioxane (*n* = 8, X = H), which has H–Si groups at the vertices of a cube with oxygen atoms bridging along the edges. In the crystalline phase octahydridosilsesquioxane has been characterized by several X-ray and neutron diffraction

\* Corresponding author. E-mail: d.w.h.rankin@ed.ac.uk.

<sup>†</sup> University of Edinburgh.

<sup>‡</sup> Imperial College London.

(1) Ionescu, T. C.; Qi, F.; McCabe, C.; Striolo, A.; Kieffer, J.; Cummings, P. T. *J. Phys. Chem. B* **2006**, *110*, 2502.

(2) Lee, A.; Lichtenhan, J. D. *J. Appl. Polym. Sci.* **1999**, *73*, 1993.

(3) Schwab, J. J.; Lichtenhan, J. D. *Appl. Organomet. Chem.* **1998**, *12*, 707.

(4) Feher, F. J.; Newman, D. A.; Walzer, J. F. *J. Am. Chem. Soc.* **1989**, *111*, 1741.

(5) Feher, F. J.; Walzer, J. F. *Inorg. Chem.* **1991**, *30*, 1689.

(6) Duchateau, R.; Abbenhuis, H. C. L.; van Santen, R. A.; Meetsma, A.; Thiele, S. K. H.; van Tol, M. F. H. *Organometallics* **1998**, *17*, 5663.

(7) Naka, K.; Itoh, H.; Chujo, Y. *Nano Lett.* **2002**, *2*, 1183.

(8) Carroll, J. B.; Frankamp, B. L.; Srivastava, S.; Rotello, V. M. *J. Mater. Chem.* **2004**, *14*, 690.

(9) Kim, K.-M.; Keum, D.-K.; Chujo, Y. *Macromolecules* **2003**, *36*, 867.

(10) Kim, B.-S.; Mather, P. T. *Macromolecules* **2002**, *35*, 8378.

(11) Leu, C.-M.; Chang, Y.-T.; Wei, K.-H. *Macromolecules* **2003**, *36*, 9122.

(12) Leu, C.-M.; Chang, Y.-T.; Wei, K.-H. *Chem. Mater.* **2003**, *15*, 3721.

(13) Zhang, C.; Bunning, T. J.; Laine, R. M. *Chem. Mater.* **2001**, *13*, 3653.

(14) Mehl, G. H.; Saez, I. M. *Appl. Organomet. Chem.* **1999**, *13*, 261.

(15) Kim, K.-M.; Chujo, Y. *J. Polym. Sci., Part A: Polym. Chem.* **2001**, *39*, 4035.

(16) Nyman, M. D.; Desu, S. B.; Peng, C. H. *Chem. Mater.* **1993**, *5*, 1636.

(17) Neumann, D.; Fisher, M.; Tran, L.; Matisons, J. G. *J. Am. Chem. Soc.* **2002**, *124*, 13998.

(18) Mengel, C.; Meyer, W. H.; Wegner, G. *Macromol. Chem. Phys.* **2001**, *202*, 1138.

(19) Ropartz, L.; Foster, D. F.; Morris, R. E.; Slawin, A. M. Z.; Cole-Hamilton, D. J. *J. Chem. Soc., Dalton Trans.* **2002**, 1997.

(20) (a) Lichtenhan, J. D. *Comments Inorg. Chem.* **1995**, *17*, 115. (b) Provatas, A.; Matisons, J. G. *Trends Polym. Sci.* **1997**, *5*, 327. (c) Zheng, L.; Hong, G.; Cardoe, E.; Burgaz, E.; Gido, S. P.; Coughlin, E. B. *Macromolecules* **2004**, *37*, 8606. (d) Li, G.; Wang, L.; Ni, H.; Pittman, C. U. *J. Inorg. Organomet. Polym.* **2002**, *11*, 123. (e) Pittman, C. U., Jr.; Li, G.-Z.; Ni, H. *Macromol. Symp.* **2003**, *196*, 301. (f) Phillips, S. H.; Haddad, T. S.; Tomczak, S. J. *Curr. Opin. Solid State Mater. Sci.* **2004**, *8*, 21. (g) Joshi, M.; Butola, B. S. *J. Macromol. Sci., Polym. Rev.* **2004**, *C44*, 389. (h) Li, G.; Pittman, C. U. *Macromol. Containing Met. Like Eleme.* **2005**, *4*, 79. (Group IVA Polymers). (i) Laine, R. M. *J. Mater. Chem.* **2005**, *15*, 3725. (j) Kannan, R. Y.; Salacinski, H. J.; Butler, P. E.; Seifalian, A. M. *Acc. Chem. Res.* **2005**, *38*, 879. (k) Bourbigot, S.; Duquesne, S.; Jama, C. *Macromol. Symp.* **2006**, *233*, 180.

(21) Shockey, E. G.; Bolf, A. G.; Jones, P. F.; Schwab, J. J.; Chaffee, K. P.; Haddad, T. S.; Lichtenhan, J. D. *Appl. Organomet. Chem.* **1999**, *13*, 311.

(22) Mellot-Draznieks, C.; Girard, S.; Férey, G. *J. Am. Chem. Soc.* **2002**, *124*, 15326.

(23) Lickiss, P. D.; Rataboul, F. *Adv. Organomet. Chem.* **2008**, *57*, 1.

**Table 1.** Calculated Geometrical Parameters for Si<sub>8</sub>O<sub>12</sub>H<sub>8</sub>, **1**<sup>a</sup>

	rSi–O	rSi–H	∠Si–O–Si
RHF/6-31G(d) <sup>a</sup>	162.6	145.2	149.4
MP2/6-31G(d) <sup>a</sup>	164.8	146.4	147.8
MP2/6-311++G(d,p) <sup>a</sup>	164.2	146.0	148.8
MP2/6-311++G(3df,3pd) <sup>a</sup>	162.9	145.3	147.8
B3LYP/6-311++G(d,p) <sup>a</sup>	164.4	146.0	149.1
B3LYP/6-311++G(3df,3pd) <sup>a</sup>	162.9	145.8	148.0
PW-DFT PBE <sup>a</sup>	164.7	147.2	146.9
RHF/cc-pVDZ <sup>b,c</sup>	165.0	146.2	148.7
RPBE/DNP <sup>c</sup>	165.4	146.7	146.8
PW-DFT (VASP) <sup>b</sup>	163.0	146.3	146.7
MM/CTR <sup>d</sup>	162.0	147.6	146.8
MM/UFF <sup>d</sup>	160.0	146.4	147.0
MM/COMPASS <sup>d</sup>	162.4	147.3	148.2
MM/HC <sup>d</sup>	163.8	147.6	146.9
MM/HC w/o <sup>d</sup>	163.8	147.6	146.9
neutron (29 K) <sup>e</sup>	162.6(2)	146.1(5)	147.35(12)

<sup>a</sup> This work. Distances are in pm, angles are in deg. Coordinates are given in Tables S2–S8. <sup>b</sup> See ref 50. <sup>c</sup> See ref 51. <sup>d</sup> See ref 1. <sup>e</sup> See ref 25.

studies,<sup>24,25</sup> in which the molecule has been shown to have  $T_h$  symmetry. However, in solution-phase studies  $O_h$  symmetry has been inferred from <sup>1</sup>H and <sup>29</sup>Si NMR spectra, which each consist of a single peak<sup>26</sup> (although this in itself does not eliminate  $T_h$  symmetry), and IR and Raman studies<sup>27</sup> that “are compatible” with the  $O_h$  point group. In addition to these experimental studies, a range of computational studies have been carried out (see Table 1) in order to determine both the structural parameters and electronic nature of POSS compounds.

Despite this significant body of previous work, no experimental gas-phase structure has so far been published for any member of the POSS family. Such a study would allow direct comparison of experimental and computational results and avoid the previous complications in such comparisons associated with crystal packing. Here, the structures of Si<sub>8</sub>O<sub>12</sub>H<sub>8</sub> (**1**) and Si<sub>8</sub>O<sub>12</sub>Me<sub>8</sub> (**2**) have been determined using both gas-phase electron diffraction (GED) and computational methods.

## Experimental Section

**Computational Studies.** As is often the case when commencing electron diffraction studies, series of calculations were performed using the Gaussian 03 suite of programs,<sup>28</sup> to assess how the computed molecular geometries of **1** and **2** are affected by different levels of theory and basis sets. The majority of the calculations

were carried out using the resources of the EPSRC National Service for Computational Chemistry Software.<sup>29</sup> Other calculations were performed using resources provided by the EaStCHEM research computing facility.<sup>30</sup> Calculations were initially performed using the spin-restricted Hartree–Fock (RHF) method with the 3-21G\* basis set<sup>31</sup> before further calculations were carried out using larger basis sets, namely, 6-31G(d),<sup>32</sup> 6-311+G(d),<sup>33</sup> 6-311++G(d,p), and 6-311++G(3df,3pd). Electron correlation was included using second-order Møller–Plesset perturbation theory (MP2),<sup>34</sup> and density functional theory (DFT) calculations were carried out using the hybrid functional B3LYP.<sup>35</sup> For **1** a harmonic force field was computed at the B3LYP level with the 6-311++G(d,p) basis set and was used to generate rms amplitudes of vibration using the SHRINK program.<sup>36</sup> The generation of amplitudes of vibration for use in the refinement of **2** is dealt with later.

As an electron diffraction experiment yields a time-averaged structure, in which the effects of vibrations may alter interatomic distances, it is common to compute corrections to apply to the distances. This allows a more accurate comparison between theoretical and experimental structures to be made. Here, the corrections were calculated as follows. Plane-wave density functional theory (PW-DFT) calculations for **1** were performed using the Car–Parrinello molecular dynamics (CPMD) code<sup>37</sup> using the resources of the Edinburgh Parallel Computing Centre. To model an isolated molecule using a periodic code, such as CPMD, a single molecule is simulated in a supercell large enough to minimize any interactions between the molecule and its periodic images. In the present study the Tuckerman–Poisson solver<sup>38</sup> was used to decouple the electrostatic interactions, allowing a smaller supercell of 14 Å to be used. Increasing this cell size was found to lead to changes in the total energy of less than 2 meV. The PBE exchange–correlation functional<sup>39</sup> was used, and the core–valence interaction was represented with Troullier–Martins norm-conserving pseudopotentials.<sup>40</sup> A plane-wave cutoff energy of 1600 eV was adopted for the calculations.

The equilibrium geometry of **1** was optimized, starting from the structure calculated at the B3LYP/6-311+G(d) level of theory, until the energy change per atom and maximum atomic force fell below  $1 \times 10^{-8}$  eV and 1 meV, respectively. This structure was then used to determine the correction terms by carrying out a molecular dynamics simulation. The simulation was performed in the canonical (NVT) ensemble using a chain of three Nosé–Hoover

(29) National Service for Computational Chemistry Software (NSCCS). URL <http://www.nscs.ac.uk>.

(30) EaStCHEM Research Computing Facility (<http://www.eastchem.ac.uk/rcf>). This facility is partially supported by the eDIKT initiative (<http://www.edikt.org>).

(31) (a) Binkley, J. S.; Pople, J. A.; Hehre, W. J. *J. Am. Chem. Soc.* **1980**, *102*, 939. (b) Gordon, M. S.; Binkley, J. S.; Pople, J. A.; Pietro, W. J.; Hehre, W. J. *J. Am. Chem. Soc.* **1982**, *104*, 2797. (c) Pietro, W. J.; Francl, M. M.; Hehre, W. J.; DeFrees, D. J.; Pople, J. A.; Binkley, J. S. *J. Am. Chem. Soc.* **1982**, *104*, 5039.

(32) (a) Hehre, W. J.; Ditchfield, R.; Pople, J. A. *J. Chem. Phys.* **1972**, *56*, 2257. (b) Hariharan, P. C.; Pople, J. A. *Theor. Chim. Acta* **1973**, *28*, 213. (c) Gordon, M. S. *Chem. Phys. Lett.* **1980**, *76*, 163.

(33) (a) Krishnan, R.; Binkley, J. S.; Seeger, R.; Pople, J. A. *J. Chem. Phys.* **1980**, *72*, 650. (b) McLean, A. D.; Chandler, G. S. *J. Chem. Phys.* **1980**, *72*, 5639.

(34) Møller, C.; Plesset, M. S. *Phys. Rev.* **1934**, *46*, 618.

(35) (a) Becke, A. D. *J. Chem. Phys.* **1993**, *98*, 5648. (b) Lee, C.; Yang, W.; Parr, R. G. *Phys. Rev. B* **1992**, *37*, 785. (c) Miehlich, B.; Savin, A.; Stoll, H.; Preuss, H. *Chem. Phys. Lett.* **1989**, *157*, 200.

(36) (a) Sipachev, V. A. *J. Mol. Struct. (THEOCHEM)* **1985**, *121*, 143. (b) Sipachev, V. A. *J. Mol. Struct.* **2001**, *567*, 67.

(37) CPMD, Version 3.11.1; IBM Corp., 1990–2006, MPI für Festkörperforschung, Stuttgart, 1997–2001.

(38) Martyna, G. J.; Tuckerman, M. E. *J. Chem. Phys.* **1999**, *110*, 2810.

(39) Perdew, J. P.; Burke, K.; Ernzerhof, M. *Phys. Rev. Lett.* **1996**, *77*, 3865.

(40) Troullier, N.; Martins, J. L. *Phys. Rev. B* **1991**, *43*, 1993.

(24) Calzaferri, G.; Imhof, R.; Törnroos, K. W. *J. Chem. Soc., Dalton Trans.* **1994**, 3123.

(25) Törnroos, K. W. *Acta Crystallogr., Sect. C: Cryst. Struct. Commun.* **1994**, *C50*, 1646.

(26) Marcolli, C.; Lainé, P.; Bühler, R.; Calzaferri, G.; Tomkinson, J. *J. Phys. Chem. B* **1997**, *101*, 1171.

(27) Baertsch, M.; Bornhauser, P.; Calzaferri, G.; Imhof, R. *J. Phys. Chem.* **1994**, *98*, 2817.

(28) Frisch, M. J.; Trucks, G. W.; Schlegel, H. B.; Scuseria, G. E.; Robb, M. A.; Cheeseman, J. R.; Montgomery, J. A., Jr.; Vreven, T.; Kudin, K. N.; Burant, J. C.; Millam, J. M.; Iyengar, S. S.; Tomasi, J.; Barone, V.; Mennucci, B.; Cossi, M.; Scalmani, G.; Rega, N.; Petersson, G. A.; Nakatsuji, H.; Hada, M.; Ehara, M.; Toyota, K.; Fukuda, R.; Hasegawa, J.; Ishida, M.; Nakajima, T.; Honda, Y.; Kitao, O.; Nakai, H.; Klene, M.; Li, X.; Knox, J. E.; Hratchian, H. P.; Cross, J. B.; Adamo, C.; Jaramillo, J.; Gomperts, R.; Stratmann, R. E.; Yazyev, O.; Austin, A. J.; Cammi, R.; Pomelli, C.; Ochterski, J. W.; Ayala, P. Y.; Morokuma, K.; Voth, G. A.; Salvador, P.; Dannenberg, J. J.; Zakrzewski, V. G.; Dapprich, S.; Daniels, A. D.; Strain, M. C.; Farkas, O.; Malick, D. K.; Rabuck, A. D.; Raghavachari, K.; Foresman, J. B.; Ortiz, J. V.; Cui, Q.; Baboul, A. G.; Clifford, S.; Cioslowski, J.; Stefanov, B. B.; Liu, G.; Liashenko, A.; Piskorz, P.; Komaromi, I.; Martin, R. L.; Fox, D. J.; Keith, T.; Al-Laham, M. A.; Peng, C. Y.; Nanayakkara, A.; Challacombe, M.; Gill, P. M. W.; Johnson, B.; Chen, W.; Wong, M. W.; Gonzalez, C.; Pople, J. A. *Gaussian 03, Revision C.01*; Gaussian, Inc.: Wallingford, CT, 2004.

thermostats<sup>41,42</sup> to regulate the simulation temperature at 400 K, approximately the temperature of the experiment. A thermostat frequency of 2400 cm<sup>-1</sup> was adopted. The simulation was run using the Car–Parrinello formulism<sup>43</sup> with an electronic time step of 75.57 as. The geometry was sampled every 15 steps, and data were collected for a total of 16 ps.

A distance,  $r_a$ , obtained directly from a GED experiment represents the inverse of the vibrationally averaged inverse of the distance between atoms  $i$  and  $j$ . This can be calculated directly from the MD simulation using

$$r_{a,ij} = \left( \frac{1}{N} \sum_{k=1}^N (r_{ij,k})^{-1} \right)^{-1}$$

where  $N$  is the total number of steps and  $r_{ij,k}$  is the separation of the  $i$ th and  $j$ th atoms at the  $k$ th step in the trajectory. The corrections used in the GED refinement were simply  $(r_a - r_e)$ , derived for each atom pair as described above.

Similar simulations were carried out for **2**. A larger cell of 15 Å together with a plane-wave cutoff of 1350 eV was used for these simulations. The equilibrium geometry was optimized to the same level of convergence as **1**. The simulation temperature of 493 K was controlled using a chain of three Nosé–Hoover thermostats with a thermostating frequency of 3500 cm<sup>-1</sup>, reflecting the presence of the higher frequency C–H stretches. A time step of 100.76 as was used. The molecular geometry was sampled every 5 CPMD steps and the simulation was run for 14 ps.

For **2** SHRINK<sup>36</sup> gives amplitudes of vibration that seem to be too large by up to 50%. This program allows for curvilinear motion with a first-order approximation, providing both amplitudes of vibration and the terms needed to correct interatomic distances as determined by electron diffraction ( $r_a$ ) to a consistent basis ( $r_{h1}$ ). Refinements were performed using the SHRINK values, and it was only when the amplitudes of vibration were refined, allowing significant changes from the calculated values, that a reasonable fit to the data was obtained. (It should be noted that even then the fit was not good enough to consider publication.) Root mean square amplitudes of vibration ( $u$ ) were therefore extracted from the simulation by obtaining the square of the difference between the instantaneous distance between atoms  $i$  and  $j$  at each time step and the average  $i$ – $j$  distance throughout the entire simulation. This was then averaged over the number of steps, then over chemically equivalent atom pairs, and finally the square root was taken as shown:

$$u_{ij} = \left( \frac{1}{N_p N_s} \sum_{s,p=1}^{N_p} \sum_{k=1}^{N_s} (r_{ij,n,p} - \langle r_{ij,p} \rangle)^2 \right)^{0.5}$$

where  $N_s$  and  $N_p$  are the number of steps and number of equivalent pairs, respectively, and

$$\langle r_{ij,p} \rangle = \frac{1}{N_s} \sum_{k=1}^{N_s} r_{ij,p}$$

The only exception to this procedure was for the C–H bonded distance, where the MD method gave an amplitude of vibration of 3.5 pm. Experience suggests, however, that this value is only about half of what is normal for such a bonded distance. That MD gets this wrong is expected, as, even at 493 K, the high-frequency C–H stretch will be affected by quantum-mechanical tunneling. The dynamics of the nuclei in an MD simulation are still treated in a

classical fashion even with the quantum-mechanics-derived forces. For the light hydrogen atom this will lead to a significant underestimation of the C–H stretching motion. For this reason the C–H amplitude was substituted with a standard value of 7.5 pm. The motion of the heavier atoms is sufficiently approximated by the classical dynamics. Furthermore, as the amplitudes of vibration for the H...X atom pairs are dominated by heavy-atom motion, these values are much less affected by quantum tunneling than C–H.

**Gas Electron Diffraction.** Data were collected for both **1** and **2** using the Edinburgh gas-phase electron diffraction (GED) apparatus<sup>44</sup> with an accelerating voltage of 40 kV (equivalent to an electron wavelength of approximately 6.0 pm). For each compound experiments were performed at two different nozzle-to-film distances to maximize the range of scattering data available. The scattering intensities were recorded on Kodak Electron Image films, and nozzle-to-film distances and nozzle and sample temperatures are given in Table S1. The camera distances were calculated using diffraction patterns of benzene recorded immediately after each sample run. The scattering intensities were measured using an Epson Expression 1680 Pro flatbed scanner and converted to mean optical densities using a method described elsewhere.<sup>45</sup> The data were then reduced and analyzed using the ed@ed least-squares refinement program<sup>46</sup> employing the scattering factors of Ross et al.<sup>47</sup> The weighting points for the off-diagonal weight matrix, correlation parameters, and scale factors are shown in Table S1.

The GED refinement procedures used here for both **1** and **2** give interatomic distances that we have termed  $r_{e,MD}$ , indicating that corrections of the form  $r_a - r_e$  have been determined from MD simulations as described above. The details of this molecular dynamics method will be published elsewhere.<sup>48</sup> Additionally, the calculated amplitudes of vibration used as starting values in the refinement of **2** were taken from MD simulations and are termed  $u_{MD}$ .

**Preparation of (Si<sub>8</sub>O<sub>12</sub>H<sub>8</sub>) and (Si<sub>8</sub>O<sub>12</sub>Me<sub>8</sub>).** The Si<sub>8</sub>O<sub>12</sub>H<sub>8</sub> was prepared as described,<sup>49</sup> and the Si<sub>8</sub>O<sub>12</sub>Me<sub>8</sub> was purchased from the Aldrich Chemical Co. and further purified by vacuum sublimation.

## Results and Discussion

**Computational Studies.** Table 1 details the results of geometry optimizations performed using various basis sets and levels of theory, together with prominent theoretical results from the literature and experimental distances from neutron diffraction experiments.<sup>25</sup> In the crystalline phase the molecular symmetry is reduced from  $O_h$  to  $T_h$ , so the experimental results given are the average values quoted in the paper.

One obvious pattern shown in Table 1 is that on introducing electron correlation, through either the MP2 or the DFT (B3LYP) method, the bond lengths increase relative to those calculated using the Hartree–Fock (RHF) method. Another is that the MP2 and B3LYP calculations show good agreement when used with equivalent basis sets. Increasing the size of the

(44) Huntley, C. M.; Laursen, G. S.; Rankin, D. W. H. *J. Chem. Soc., Dalton Trans.* **1980**, 954.

(45) Fleischer, H.; Wann, D. A.; Hinchley, S. L.; Borisenko, K. B.; Lewis, J. R.; Mawhorter, R. J.; Robertson, H. E.; Rankin, D. W. H. *Dalton Trans.* **2005**, 3221.

(46) Hinchley, S. L.; Robertson, H. E.; Borisenko, K. B.; Turner, A. R.; Johnston, B. F.; Rankin, D. W. H.; Ahmadian, M.; Jones, J. N.; Cowley, A. H. *Dalton Trans.* **2004**, 2469.

(47) Ross, A. W.; Fink, M.; Hilderbrandt, R. *International Tables for Crystallography*; Wilson, A. J. C., Ed.; Kluwer Academic Publishers: Dordrecht, The Netherlands, 1992; Vol. C, p245.

(48) Wann, D. A.; Reilly, A. M.; McCaffrey, P. D.; Rankin, D. W. H. Manuscript in preparation.

(49) Agaskar, P. Y. *Inorg. Chem.* **1991**, 30, 2707.

(41) Hoover, W. G. *Phys. Rev. A* **1985**, 31, 1695.

(42) Nosé, S. *J. Chem. Phys.* **1984**, 81, 511.

(43) Car, R.; Parrinello, M. *Phys. Rev. Lett.* **1985**, 55, 2471.

**Table 2. Refined  $r_{e,MD}$  Parameters from the GED Refinement for  $\text{Si}_8\text{O}_{12}\text{H}_8$ , **1**<sup>a</sup>**

independent parameter		$r_{e,MD}$	$r_e^b$	restraint
$p_1$	$r_{\text{Si-O}}$	161.41(3)	162.9	
$p_2$	$r_{\text{Si-H}}$	145.4(8)	145.3	145.3(10)
$p_3$	$\angle\text{Si-O-Si}$	147.9(2)	147.8	

<sup>a</sup> Distances are in pm, angles are in deg. The numbers in parentheses are estimated standard deviations of the last digits. <sup>b</sup> Theoretical results from MP2/6-311++G(3df,3pd) calculations.

basis set from double- $\zeta$  to triple- $\zeta$  quality has a modest effect on the calculated bond lengths at the MP2 level, decreasing the Si-O bond length by 0.6 pm and Si-H by 0.4 pm. However, augmenting the basis set with orbitals of higher angular momentum [6-311++G(3df,3pd)] has a more pronounced effect, decreasing the Si-O bond length by a further 1.3 pm using the MP2 method and 1.5 pm using the B3LYP method. Adding further polarization functions onto the hydrogen atoms obviously has little effect on the Si-O bond but does further decrease the Si-H bond length.

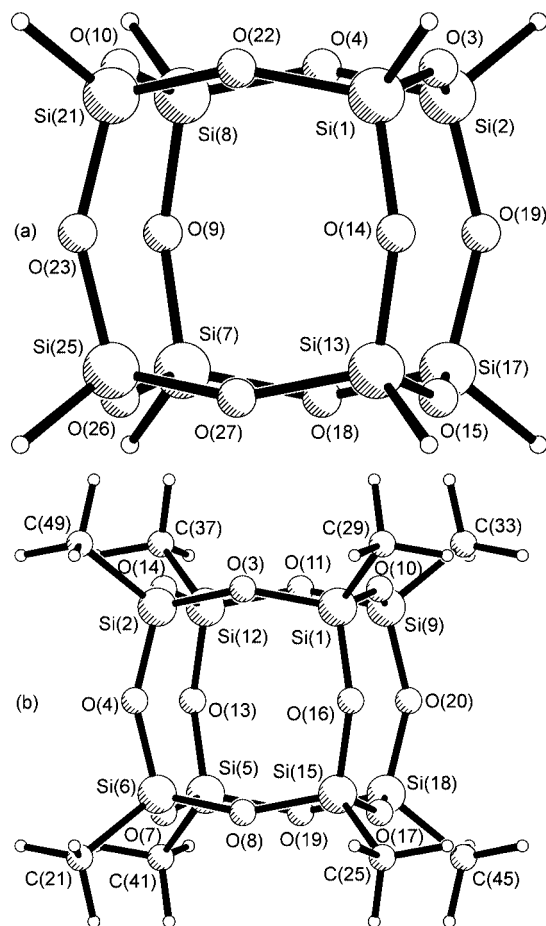
The significant differences observed on changing methods and basis sets is also evident in the literature. McCabe et al.<sup>50</sup> reported a much longer Si-O distance (165.0 pm) from their calculations on **1** using the HF method and a double- $\zeta$  basis set (RHF/cc-pVDZ). They also report a DFT calculation using the revised Perdew-Burke-Ernzerhof (RPBE) generalized gradient approximation and the all-electron double-numerical-polarized (DNP) basis set.<sup>51</sup> This calculation predicts an even longer Si-O distance (165.4 pm). The average distances obtained from the neutron diffraction studies by Törnroos<sup>25</sup> agree with the highest-level isolated-molecule calculations to within two standard deviations for the Si-O distance and to within one standard deviation for the Si-H distance, although the Si-O-Si angle is calculated to be around 0.5° wider (4 standard deviations).

For comparison, our PW-DFT calculation, in the large supercell, gives bond lengths 1.8 pm longer for  $r_{\text{Si-O}}$  and 1.4 pm longer for  $r_{\text{Si-H}}$  compared to B3LYP/6-311++G(3df,3pd). As expected MM methods give more varied results, although they are of reasonable accuracy when compared to the *ab initio* methods.

**GED Refinements.** A molecular model was written for **1** to allow the refinable geometrical parameters to be converted into Cartesian coordinates. The high symmetry of the molecule ( $O_h$ ) allowed the geometry to be described using only three parameters, namely, the Si-O and Si-H bonded distances ( $p_{1-2}$ ) and the Si-O-Si angle ( $p_3$ ) (see Table 2). See Figure 1a for a picture of the molecular structure complete with atom numbering.

A similar  $O_h$ -symmetric model to that used for **1** was written to describe the geometry of **2**. Table 3 shows that in this case two extra parameters were required for the methyl groups, which were assumed to have  $C_{3v}$  local symmetry. On the basis of calculations described above it was assumed that the methyl groups were staggered. The molecular structure of **2** is shown in Figure 1b.

The initial geometries for the refinements of the structures of **1** and **2** were taken from the MP2/6-311++G(3df,3pd) calculations. Starting values for the root mean square (rms) amplitudes of vibration were obtained using methods described

**Figure 1.** Molecular structures of (a)  $\text{Si}_8\text{O}_{12}\text{H}_8$ , **1**, and (b)  $\text{Si}_8\text{O}_{12}\text{Me}_8$ , **2**, including atom numbering.**Table 3. Refined  $r_{e,MD}$  Parameters from the GED Refinement for  $\text{Si}_8\text{O}_{12}\text{Me}_8$ , **2**<sup>a</sup>**

independent parameter		$r_{e,MD}$	$r_e^b$	$r_e^c$	X-ray <sup>d</sup>	restraint
$p_1$	$r_{\text{Si-O}}$	161.74(5)	163.2	162.9	161.4(2)	
$p_2$	$r_{\text{Si-C}}$	182.9(3)	183.7	185.3	182.7(5)	
$p_3$	$r_{\text{C-H}}$	110.1(7)	108.9	108.6	87.5(30)	108.9(10)
$p_4$	$\angle\text{Si-O-Si}$	148.9(2)	148.6	149.9	149.2(5)	
$p_5$	$\angle\text{Si-C-H}$	110.9(7)	110.5	110.8		110.5(10)

<sup>a</sup> Distances are in pm, angles are in deg. The numbers in parentheses are estimated standard deviations of the last digits. <sup>b</sup> Theoretical results from MP2/6-311++G(3df,3pd) calculations. Coordinates and energy are given in Table S9. <sup>c</sup> Theoretical results from RHF/6-31G\*\* calculations, ref 52. <sup>d</sup> Average experimental values from an X-ray crystallographic study.<sup>53</sup>

above, as were the corrections to give bonded distances of the type  $r_{e,MD}$ . The least-squares refinement processes were carried out using the ed@ed software.<sup>46</sup>

For the refinement of **1** a flexible SARACEN restraint<sup>54</sup> was applied to the Si-H bond length using the calculated value [MP2/6-311++G(3df,3pd)] and an uncertainty of 1 pm, as it could not be refined sensibly because of the lack of information regarding the positions of hydrogen atoms. Root mean square amplitudes of vibration (RDC) were restrained by ratios fixed at the calculated values. A full list of the amplitudes of vibration and their corresponding distances is

(50) McCabe, C.; Glotzer, S. C.; Kieffer, J.; Neurock, M.; Cummings, P. T. *J. Comput. Theor. Nanosci.* **2004**, *1*, 265.

(51) Li, H.-C.; Lee, C.-Y.; McCabe, C.; Striolo, A.; Neurock, M. *J. Phys. Chem. A* **2007**, *111*, 3577.

(52) Shen, J.; Cheng, W.-D.; Wu, D.-S.; Li, X.-D.; Lan, Y.-Z.; Zhang, H.; Gong, Y.-J.; Li, F.-F.; Huang, S.-P. *J. Chem. Phys.* **2005**, *122*, 204709.

(53) Koellner, G.; Müller, U. *Acta Crystallogr.* **1989**, *C45*, 1106.

(54) (a) Blake, A. J.; Brain, P. T.; McNab, H.; Miller, J.; Morrison, C. A.; Parsons, S.; Rankin, D. W. H.; Robertson, H. E.; Smart, B. A. *J. Phys. Chem.* **1996**, *100*, 12280. (b) Brain, P. T.; Morrison, C. A.; Parsons, S.; Rankin, D. W. H. *J. Chem. Soc., Dalton Trans.* **1996**, 4589. (c) Mitzel, N. W.; Rankin, D. W. H. *Dalton Trans.* **2003**, 3650.

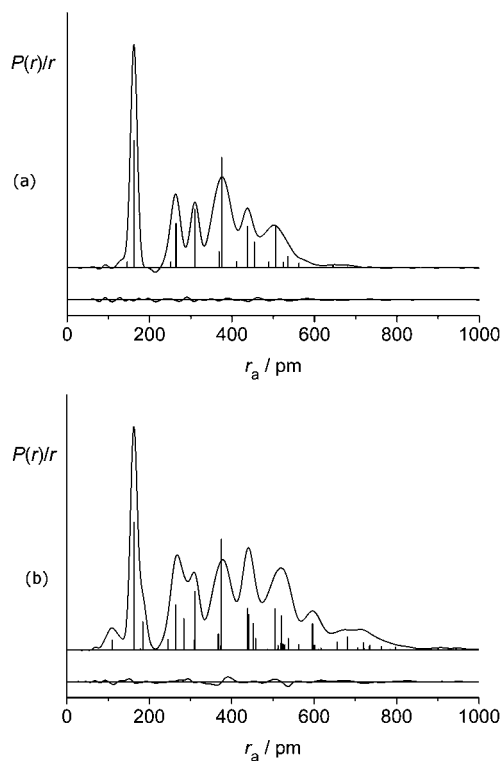


**Figure 2.** Experimental and difference (experimental minus theoretical) radial-distribution curves,  $P(r)/r$ , for (a)  $\text{Si}_8\text{O}_{12}\text{H}_8$ , **1**, and (b)  $\text{Si}_8\text{O}_{12}\text{Me}_8$ , **2**. Before Fourier inversion the data were multiplied by  $s \exp(-0.00002s^2)/(Z_{\text{Si}} - f_{\text{Si}})(Z_{\text{O}} - f_{\text{O}})$ .

given in Table S10. A further flexible restraint was applied to  $u_{15}$  [Si(1)⋯Si(7)], using an uncertainty of 10% of the absolute computed value. With these restraints in place all parameters and many significant rms amplitudes of vibration were refined. The final  $R_G$  factor for the fit between the theoretical scattering (generated from the model) and the experimental data for **1** was 0.051 ( $R_D = 0.032$ ). The final RDC is shown in Figure 2a, and the corresponding molecular-intensity scattering curves are shown in Figure S1. Coordinates for the final structure are given in Table S11, and the least-squares correlation matrix is in Table S12.

For **2** restraints were applied to the C–H distance and the Si–C–H angle and to  $u_1$ , the C–H amplitude of vibration. All other parameters and most amplitudes of vibration were then refined, giving a final  $R$  factor of 0.077 ( $R_D = 0.054$ ). A full list of the amplitudes of vibration and their corresponding distances is given in Table S13. The radial-distribution curves and molecular-intensity scattering curves are shown in Figure 2b and Figure S2, respectively. Coordinates for the final structure are given in Table S14, and the least-squares correlation matrix is in Table S15.

The structure of the methyl derivative, **2**, has been the subject of far fewer studies than that of **1**, but some theoretical data are included in Table 3 for comparison. The solid-state structure of **2** was also the subject of an X-ray crystallographic study, which showed the Si–O bond lengths to fall in the range 161.0(2)–161.7(2) (mean 161.4) pm and Si–O–Si angles of 148.9(1)–149.6(5) (mean 149.2°).<sup>53</sup> These are not significantly different from the parameters found in the gas phase (although the C–H bond distance of 87.5 pm found in the solid state is very short, even for an X-ray study). One must also remember that GED yields the distances between nuclei, while X-ray diffraction gives distances between centers of electron density, and so any direct comparisons must be made with caution. When considering these X-ray values, it should be noted that an unpublished X-ray structure of **2** has been deposited in the Cambridge Structural Database

(reference OCMSIO02).<sup>55</sup> Unfortunately, no details are given of how this refinement differs from that in ref 53. It appears to give essentially the same structure but with more reasonable values for the CH distances (around 0.98 pm; uncertainty unknown). We think that it is likely that the unpublished structure has taken account of the freely rotating methyl group and corrected the hydrogen positions accordingly.

The narrow range in the Si–O–Si angles in the published crystal structure is much smaller than in many alkyl-substituted POSS compounds in the solid state. For example, in  $\text{Si}_8\text{O}_{12}(n\text{-C}_8\text{H}_{17})_8$  the Si–O–Si angles fall in the range 141.1–159.8°<sup>56</sup> and in  $\text{Si}_8\text{O}_{12}[(\text{CH}_2)_3\text{Br}]_8$  in the range 141.7(4)–153.8(5)°,<sup>57</sup> although the average values, 149.3° and 148.8°, respectively, fall close to the 148.9(2)° found in **2** and the 147.9(2)° in **1**. A wide range of  $\text{Si}_8\text{O}_{12}\text{X}_8$  compounds have been found to have average Si–O–Si angles of 147–150° in the solid state,<sup>23</sup> and the gas-phase structures for **1** and **2**, for which crystal packing is irrelevant, clearly fall into the same range. The solid-state distortions of the polyhedral  $\text{Si}_8\text{O}_{12}$  cores substituted by larger, more flexible substituents are presumably caused by the substituents adopting conformations that minimize the voids that would be present in the structure if they were to point ideally toward the vertices of a cube. The larger POSS molecules distort either by substituents on two opposite faces of the core closing up toward each other to form a disk-like structure or the substituents around a pair of opposite faces closing up around these faces to provide a more rod-like geometry. These distortions are much less favorable with the small, rigid substituents used in this study. POSS structures are discussed in more detail in ref 23.

## Conclusions

This work provides the first detailed experimental data on the structures of polyhedral silsesquioxanes in the gas phase and has enabled comparisons with calculated structures on single POSS molecules to be made. Calculations at the MP2/6-311++G(3df,3pd) level reproduce the gas-phase experimental data for  $\text{Si}_8\text{O}_{12}\text{H}_8$  and  $\text{Si}_8\text{O}_{12}\text{Me}_8$  well.

**Acknowledgment.** We thank Prof. Paul Madden for useful discussions. The EPSRC is acknowledged for funding the electron diffraction research in Edinburgh (EP/C513649) and the related visit of F.R. to Edinburgh, and for funding R.L. (EP/C528816/1) at Imperial College London. We thank the UK Energy Research Centre for funding F.R. P.D.M. and A.M.R. thank the School of Chemistry, University of Edinburgh, for funding studentships. The NSCCS, EaStCHEM research computing facility, and Edinburgh Parallel Computing Centre provided valuable computational hardware and software.

**Supporting Information Available:** Tables of experimental parameters for the GED analysis of **1** and **2** (Table S1), calculated coordinates using a variety of methods and basis sets for **1** (Tables S2–S8) and for **2** (Table S9), refined and calculated rms amplitudes of vibration ( $u$ ), associated  $r_a$  distances, and corresponding perpendicular correction values ( $k$ ) (Table S10), GED-determined atomic coordinates (Table S11), and least-squares correlation matrix (Table S12) for **1**, and the same for **2** (Tables S13–S15). Molecular-intensity scattering and difference curves for **1** and **2** (Figures S1 and S2). This material is available free of charge via the Internet at <http://pubs.acs.org>.

OM800357T

(55) Bolte, M. Private communication, Cambridge Structural Database, reference OCMSIO02.

(56) Bassindale, A. R.; Chen, H.; Lui, Z.; MacKinnon, I. A.; Parker, D. J.; Taylor, P. G.; Yang, Y.; Light, M. E.; Horton, P. N.; Hursthouse, M. B. *J. Organomet. Chem.* **2004**, *689*, 3287.

(57) Lucke, S.; Stoppek-Langner, K.; Krebs, B.; Lage, M. *Z. Anorg. Allg. Chem.* **1997**, *623*, 1243.